Supplementary Materials for

Finite perovskite hierarchical structures via ligand confinement leading to efficient inverted perovskite solar cells

Yanchun Huang[1], Kangrong Yan[1], Benfang Niu[1], Zeng Chen[2], Emely Gu[3], Haoran Liu[1], Buyi Yan[3], Jizhong Yao[3], Haiming Zhu[2], Hongzheng Chen[1], Chang-Zhi Li[1]*

[1]State Key Laboratory of Silicon Materials, MOE Key Laboratory of Macromolecular Synthesis and Functionalization, Department of Polymer Science and Engineering, Zhejiang University, Hangzhou 310027, P. R. China.

[2]Department of Chemistry, Zhejiang University, Hangzhou 310027, P. R. China.

[3]Hangzhou Microquanta Semiconductor Co. LTD. No. 7 Longtan Road, Innovation Park, Hangzhou 310027, P. R. China.

*Corresponding author. Email: czli@zju.edu.cn.

Materials and Methods

Instrument Information

Proton nuclear magnetic resonance (^{1}H NMR) spectra was characterized by a Bruker Advance III 400 (400 MHz) NMR instrument. Electron spin-resonance spectroscopy (ESR) was characterized by a Bruker A300 X-band ESR spectrometer. Fourier transform infrared (FT-IR) spectra were recorded on a JASCO model FT-IR-6100 infrared spectrometer. UV-vis absorption spectra were recorded on a Shimadzu UV-2450 spectrophotometer. The field-emission scanning electron microscope (FESEM) measurements were carried out on Hitachi S-4800, and SEM samples were fabricated with the architecture of ITO/HTL/perovskite. The X-ray photoelectron spectroscopy (XPS) experiments was performed on AXIS Supra (Kratos). Time-of-Flight Secondary Ion Mass Spectrometry (TOF-SIMS) Measurements. Cs^+ was used as the sputter source with a 500 eV energy and 40 nA current on IONTOF TOF-SIMS 5-100. The photoluminescence (PL) and transient photoluminescence (TRPL) spectra were recorded on a PTI QM-40 spectrofluorometer with an excitation wavelength of 480 nm and a Horiba DeltaFlex modular lifetime measurement system patented TCSPC technique, respectively. Grazing incidence wide angle X-ray scattering (GIWAXS) measurements were collected using a Xeuss 3.0 spectrometer with high brightness microfocal spot solid Cu target as the X-ray source and Eiger 2R 1M as the detector. The sample-to-detector distance was 100 mm. The surface potential was measured by

KPFM (Bruker Dimension Icon) under dark conditions without applied bias.

Materials

Unless stated otherwise, all materials and solvents were purchased from Sigma-Aldrich and used as received. Nickel (II) nitrate hexahydrate ($Ni(NO_3)_2.6H_2O$, 98.0%) and ethylene diamine (99%) were purchased from Alfa Aesar. Lead iodide (PbI_2), formamidinium iodide (FAI), and methyl ammonium bromide (MABr) were purchased from Shanghai MaterWin New Materials. Lead bromide ($PbBr_2$) and cesium iodide (CsI) were purchased from TCI. Poly(bis(4-phenyl) (2,4,6-trimethylphenyl)amine) (PTAA), phenylethyl ammonium bromide (PEABr), methyl ammonium chloride (MACl), n-butyl ammonium bromide (BABr) and $PC_{61}BM$ (99.0%) were purchased from Xi'an p-OLED. Bathocuproine (BCP, 99%) and ethylene glycol (99.5%) were purchased from TCI.

Device Fabrication and Characterization

Small-area perovskite solar cells:

$Cs_{0.05}(FA_{0.95}MA_{0.05})_{0.95}Pb(I_{0.95}Br_{0.05})_3$-based devices

The Glass/ITO substrates were sequentially cleaned with detergent (2%vol Hellmenex), deionized water, acetone, isopropanol and ethanol by ultrasonication for 15 min in each solvent. The cleaned ITO substrates were then dried in air oven and treated with UV ozone for 20 min before use. The small-area device is based on the architecture of ITO/NiO_x/PTAA/Perovskite/PCBM/BCP/Ag. Nickel (II) nitrate hexahydrate ($Ni(NO_3)_2.6H_2O$, 5 g) and ethylenediamine (1.145 ml) were dissolved in ethtylene glycol (17.195 ml) to obtain NiO_x precursor solution. And then 185 μL KCl solution (100 mg/ml in 10 ml H_2O) was added into 10 ml NiO_x precursor solution. The KCl incorporated NiO_x solution was spin-coated on the ITO glass at 4000 rpm for 30 s and annealed at 300 ℃ for 1 hour. PTAA (1.5 mg/ml in chlorobenzene, CB) was spin-coated on the NiO_x substrate at 6000 rpm for 30 s, followed with annealing at 100 °C for 10 min. 1.4 M perovskite precursor solution is prepared in DMF: DMSO (4:1/v:v) solvent according to a formula of $Cs_{0.05}(FA_{0.95}MA_{0.05})_{0.95}Pb(I_{0.95}Br_{0.05})_3$ with 5% excess amount of PbI, and 30 mol% of MACl. 50 μL of the prepared perovskite precursor solution was spin-coated on ITO/NiO_x/PTAA substrates at 1000 rpm for 10 s and 5000 rpm for 30 s. 120 μL IPA was dripped on the substrate at 10 s prior to the end of the second procedure during spin-coating. Then the substrate was annealed at 100 °C for 30 min to obtain 3D perovskite films. EDA solution (0.1 mM in Toluene) was then spin-coated on 3D perovskite at 4000 rpm and then annealed at 70 °C for 5 min to obtain EDA/3D perovskite films. PEABr solution (2 mg/ml in IPA) was spin-coated atop of 3D perovskite films at 5000 rpm and then annealed at 100 °C for 5 min to fabricate 2D/3D perovskite films. For finite 2D/3D perovskite films, the EDA solution was deposited on the 3D perovskite surface prior to PEABr (or BABr) solution. PCBM (20 mg/ml in CB) and BCP (1 mg/ml in ethanol) were spin-coated at 3000 rpm for 30 s, respectively, followed by deposited 100 nm Ag in vacuum chamber under high vacuum of 2×10^{-4} Pa. The device area is 5.979 mm^2, which is defined by the shade mask.

For $Cs_{0.1}FA_{0.7}MA_{0.2}Pb(I_{0.55}Br_{0.45})_3$-based devices

The procedures of ITO/Glass substrate cleaning, and HTL deposit were consistent with $Cs_{0.05}(FA_{0.95}MA_{0.05})_{0.95}Pb(I_{0.95}Br_{0.05})_3$-based device fabrication. Perovskite precursor solution (1 M) was prepared in DMF: DMSO mixed solvent (3:2/v:v) and kept at 60 °C during spin-coating. 50 μL of the prepared precursor solution was spin-coated on hot substrates (60 °C) at 1000 rpm for 10 s and 6000 rpm for 30 s. 70 μL ethyl acetate was dripped on the substrate at 5 s prior to the end of the second procedure during spin-coating. Then the substrate was annealed at 100 °C for 40 min to obtain perovskite films. The procedures of EDA, PEABr, PCBM, BCP layers and metal electrode evaporation follow the description of $Cs_{0.05}(FA_{0.95}MA_{0.05})_{0.95}Pb(I_{0.95}Br_{0.05})_3$-based device fabrication.

Inverted modules:

The inverted module is based on the architecture of ITO/NiO_x/PTAA/Perovskite /PCBM/BCP/Ag. Glass substrates (6 × 6 cm^2) are provided with pre-deposited ITO layer. The cleaned glass/ITO substrate was laser scribed by a 1064 nm nano-sec beam (2 W) to form isolated cell units. 2 mg/ml PTAA solution was slot-die coated atop of NiO_x layer at a speed of 20 mm/s in air and then annealed at 100 ℃ for 10 min. The 3D perovskite film was fabricated by vacuum flash-assisted solution process. 1.4 M perovskite precursor solution dissolved in DMF: DMSO (4:1/v:v) solvent according to a formula of $Cs_{0.05}(FA_{0.95}MA_{0.05})_{0.95}Pb(I_{0.95}Br_{0.05})_3$ with 5% excess amount of PbI, and 30 mol% of MACl. 500 μL of the prepared precursor solution was spin-coated on ITO/NiO_x/PTAA substrates at 4000 rpm for 40 s and the wet film was immediately placed into a vacuum chamber for 30s by removing most of the residual solvents. Then the substrate was annealed at 100 °C for 30 min to obtain 3D perovskite films. For finite 2D/3D perovskite films, 0.1 mM EDA solution in Toluene was spin-coated on 3D perovskite film and then annealed at 70 °C for 5 min. After cooling down, PEABr (2 mg/ml in IPA) solution was spin-coated on top and then annealed at 100 °C for 5 min. After deposition of PCBM and BCP, a 532 nm nano-sec laser beam (2 W) was used for P2 scribing to expose the top ITO layer for later series connection. Ag electrode was vacuum deposited to finalize the module layer stack. P3 scribing and P4 edge isolation were carried out with the same 532 nm nano-sec beam (2 W).

Encapsulation:

Device encapsulation was carried out inside a nitrogen-filled glovebox. Copper-tin alloy belts were soldered to the electrodes of modules to extend the electric connections. UV-curable adhesive (Shanghai Mater Win New Materials) is applied to the module's edge and then the module (the metal electrode side) was fixed to the cover glass at room temperature. Finally, it was exposed to ultraviolet light (365nm, 8W) for 10 min to cure the adhesive to obtain the encapsulated module and the edges were sealed by 3M tapes.

Characterization: The *J-V* characteristics were recorded by Keithley 2400 source meter under AM 1.5G 1 sun intensity illumination (100 mW/cm^2) with the solar simulator (Enlitech, SS-F5-3A). And the light intensity was calibrated by a certified standard

silicon solar cell (SRC-2020, Enlitech). The *J-V* measurements were performed in glovebox under N_2 atmosphere with the shade mask (the area of 5.979 mm^2). The voltage step is 0.02 V, with a delay time of 1 ms/step and a scan rate of 100 mV/s, and the bias voltage is from 1.3 V to -0.1 V as reverse scanning and from -0.1 V to 1.3 V as forward scanning. The EQE spectrum was measured by a QE-R Solar Cell Spectral Response Measurement System (Enlitech). The stable PCE output were continuously measured at the voltage of maximum power point (MPP) under one-sun illumination. For the operational stability test, the encapsulated PSC devices was measured through MPP tracking under continuous 1 sun-equivalent illumination in open air with a temperature of 30 °C (100 mW/cm^2, white LED).

The *J-V* characteristic curves of modules were recorded on the Keithley source unit 2400 under AM 1.5G 1 sun intensity illumination (100 mW/cm^2) by an AAA solar simulator (SS-100A) from Beijing Sanyou Technology, and the light intensity was calibrated with a standard photovoltaic reference cell. The *J-V* measurements of PSC modules were performed in glovebox under N_2 atmosphere with the aperture area (19.30 cm^2, no shade in interconnection area). Geometrical fill factor of 97% is to define the ratio of the effective area to the aperture area of the solar module.

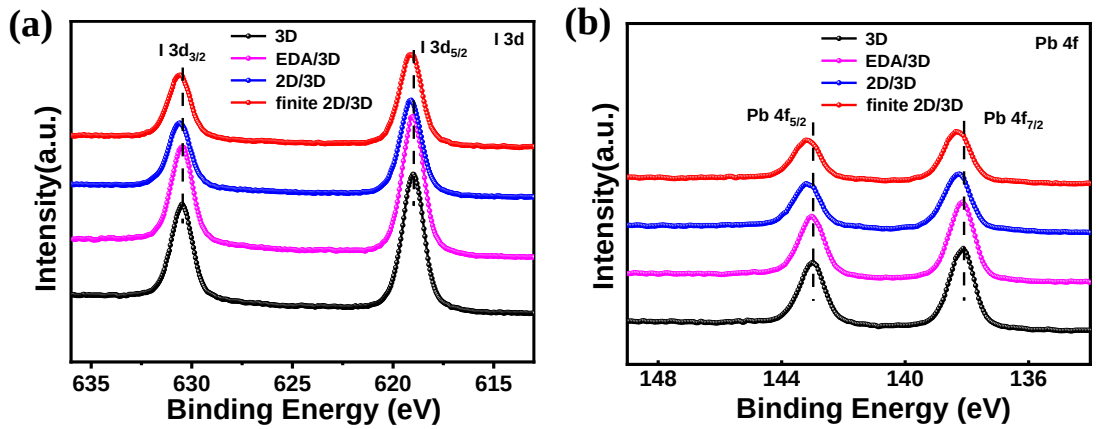

Fig. S1 XPS spectrum of I 3d (**a**) and Pb 4f (**b**) for the 3D, EDA/3D, 2D/3D and finite 2D/3D.

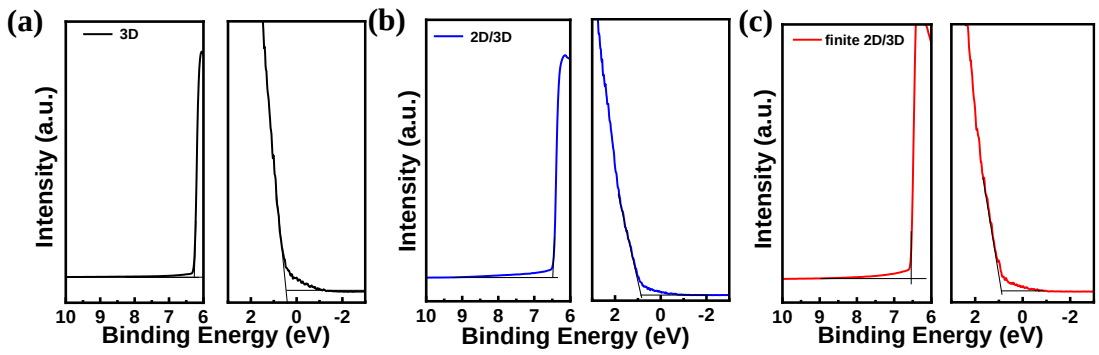

Fig. S2 UPS data for the 3D, 2D/3D and finite 2D/3D perovskite films.

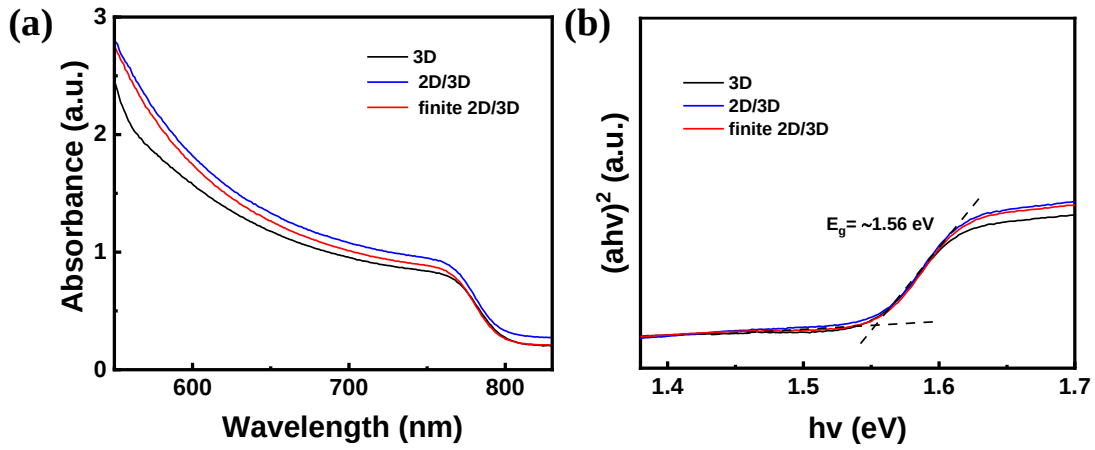

Fig. S3 (a) UV-vis absorption spectra of the 3D, EDA/3D, 2D/3D and finite 2D/3D perovskite films and (b)Tauc plot of 3D, 2D/3D and finite 2D/3D perovskite films. The optical bandgap of 3D, 2D/3D and finite 2D/3D perovskite films remains similar (~1.56 eV).

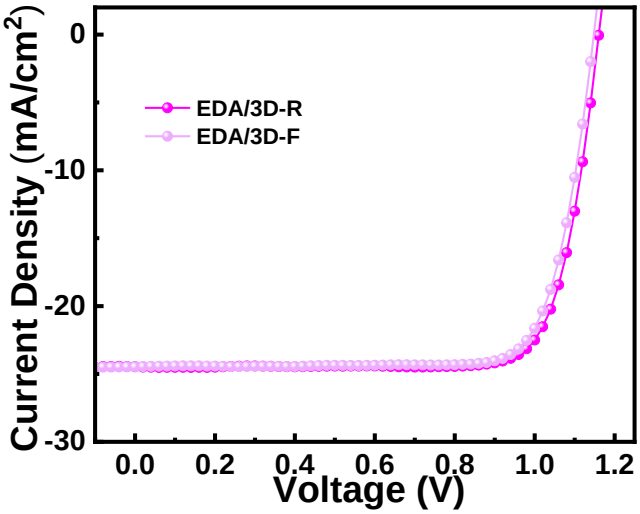

Fig. S4 *J-V* curves of the inverted PSC based on EDA/3D perovskites.

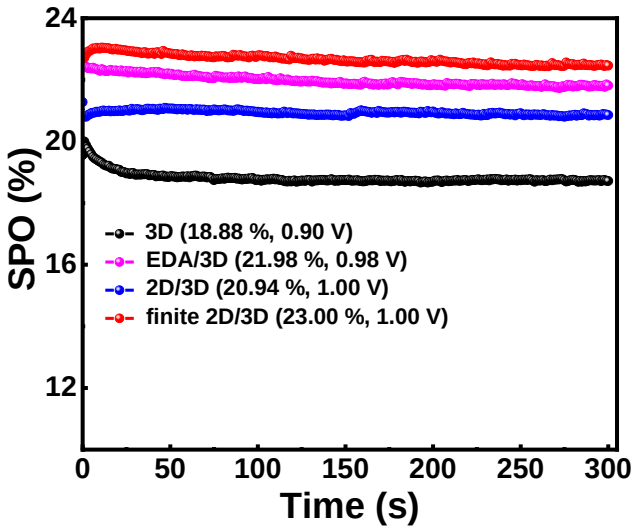

Fig. S5 The steady-state power outputs (SPO) of 3D, EDA/3D, 2D/3D and finite 2D/3D perovskite films as a function to time at the V_{max} from *J-V* scanning.

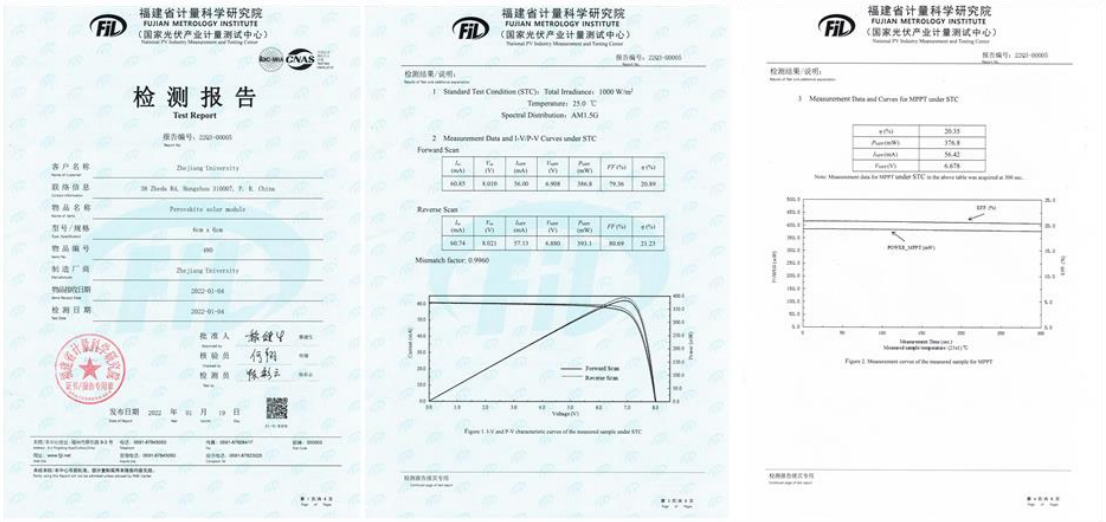

Fig. S6 The certification report for inverted modules with the shade mask (the area of 18.52 cm^2) from the Chinese National Photovoltaic Industry Metrology and Testing Center (NPVM)

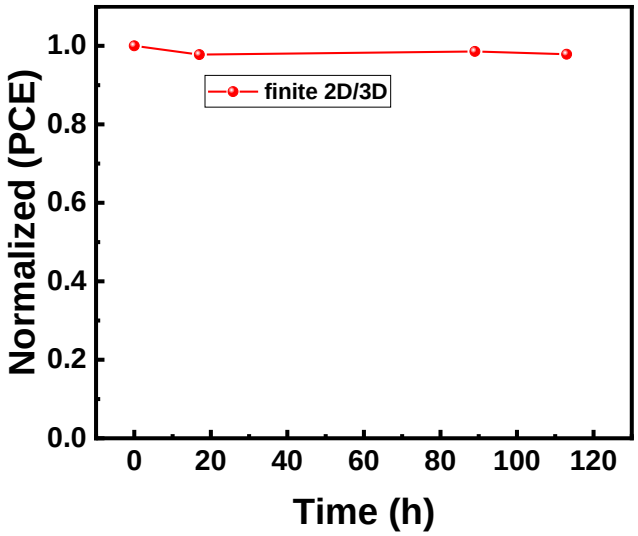

Fig.S7 Thermal stability of finite 2D/3D device under constant heating at 60 ℃ in the glove box.

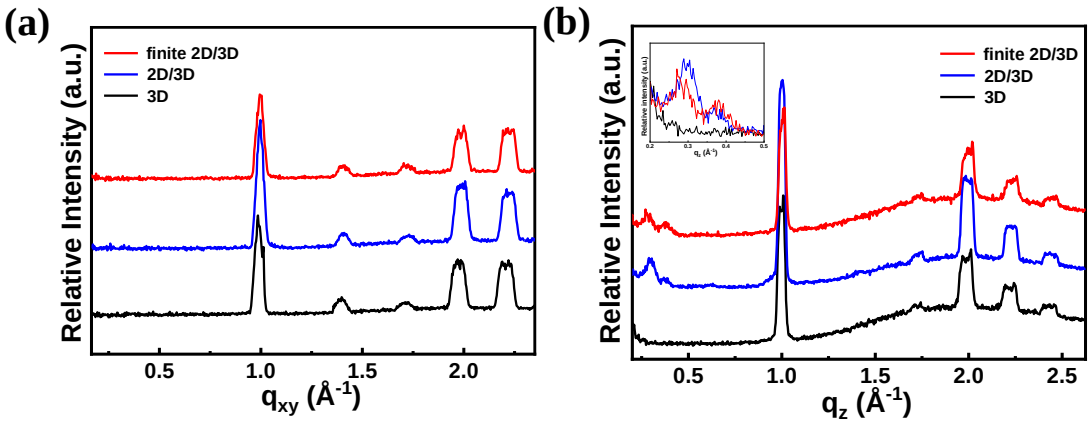

Fig. S8 In-plane (a) and out-of-plane (b) linecut profiles of 3D, 2D/3D and finite 2D/3D perovskite films.

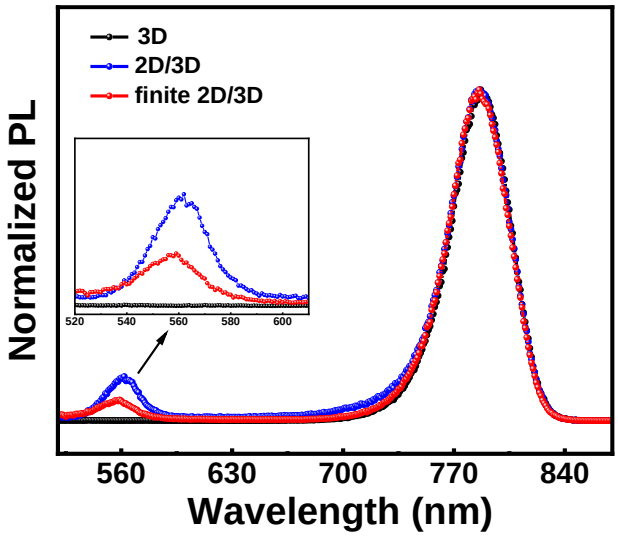

Fig. S9 Steady-state PL spectra of the corresponding perovskite films.

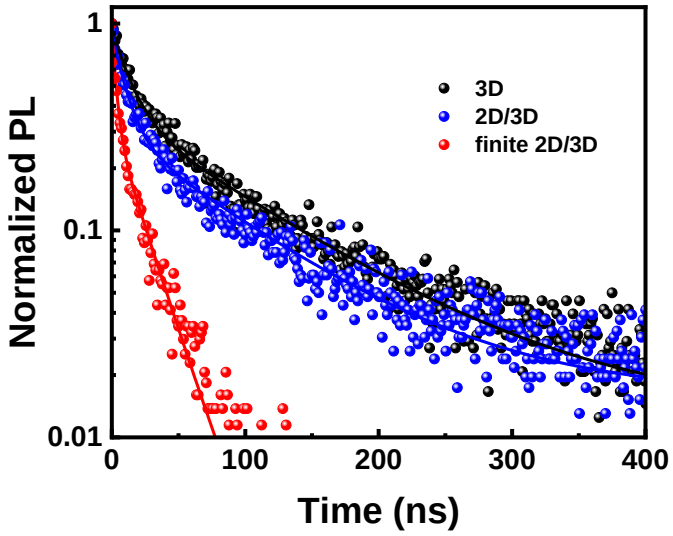

Fig. S10 Time resolution photoluminescence spectra of the corresponding perovskite films with PCBM as an electron quencher.

Table S1 Photovoltaic parameters of the mini-modules (7 sub-cells) with finite 2D/3D at reverse and forward scanning.

	Mode	V_{OC} (V)	I_{SC} (mA)	FF (%)	PCE (%)
finite 2D/3D	Reverse	7.98	63.2	80.2	21.6
	Forward	7.99	63.4	79.7	21.6

Table S2 Device performances of inverted PSCs with medium-bandgap perovskites and BABr passivation under AM 1.5G illumination (100 mW/cm^2). [a]

Sample	V_{OC} (V)	J_{SC} (mA/cm^2)	FF (%)	PCE (%)
3D	1.11 1.09±0.01	24.5 23.9±0.2	70.5 70.9±1.7	19.2 18.5±0.5
2D/3D	1.17 1.16±0.01	23.3 23.5±0.3	77.4 76.1±0.1	21.1 20.7±0.3
finite 2D/3D	1.18 1.19±0.01	24.8 24.3±0.2	81.1 80.4±0.7	23.8 23.2±0.3

[a] The average parameters with standard deviations in parentheses from 20 devices.

Table S3 Device performances of inverted PSCs with wide-bandgap perovskites and PEABr passivation under AM 1.5G illumination (100 mW/cm^2). [a]

Sample	V_{OC} (V)	J_{SC} (mA/cm^2)	FF (%)	PCE (%)
3D	1.22 1.23±0.01	18.3 17.5±0.6	80.4 78.3±0.8	18.0 16.9±0.7
2D/3D	1.25 1.24±0.01	18.1 17.6±0.4	81.4 80.5±1.0	18.4 17.6±0.3
finite 2D/3D	1.25 1.25±0.01	18.3 18.0±0.4	84.3 82.8±0.9	19.4 18.7±0.5

[a] The average parameters with standard deviations in parentheses from 20 devices.

Table S4 Parameters of time-resolved PL measurements.

Sample	τ_1 (ns)	A_1 (%)	τ_2 (ns)	A_2 (%)	τ (ns)[a]
3D	13.75	64.06	101.41	35.94	84.35
2D/3D	10.19	70.92	89.69	29.08	72.44
finite 2D/3D	3.23	66.63	21.64	33.37	17.41

[a] The average decay time can be determined as $\tau = (\Sigma A_i\tau_i^2)/(\Sigma A_i\tau_i)$.

Supporting Table. Literature reference for inverted perovskite solar modules (active areas > 10 cm^2)

Architecture	Active area(cm^2)	PCE (%)	Year	Ref.
FTO/NiO/PVSK/g-PCBM/BCP/Ag	36	15.60	2019	1
ITO/PTAA/PVSK/C60/BCP/Cu	50	19.30	2021	2
ITO/PTAA/PVSK/C60/BCP/Cu	60.80	16.30	2021	3
ITO/PTAA/PVSK/C60/BCP/Cu	35.80	18.20	2021	4
ITO/PEDOT:PSS/PVSK/PCBM/Ca/Al	25.20	14.30	2016	5
ITO/PEDOT:PSS/PVSK/PC_{71}BM/Ca/Al	11.25	15.40	2017	6
ITO/PTAA/PVSK/C60/BCP/electrode	63.70	16.40	2019	7
ITO/PEDOT:PSS/PVSK/PCBM/Au	40	12.90	2015	8
ITO/PTAA/PVSK/PC_{61}BM/BCP/Ag	10.08	15.38	2020	9
ITO/PTAA/PVSK/PC_{61}BM/BCP/Ag	25	13.45	2022	10
ITO/PEDOT:EVA/PVSK/PCBM/BCP/Ag	31.20	17.55	2020	11
ITO/PEDOT:PSS/PVSK/PCBM/LiF/Al	60	8.70	2014	12
FlexiblePET/ITO/PEDOT:GO/PVSK/PC_{61}BM/Ag	25	10.26	2021	13
ITO/PTAA/PVSK/PCBM/BCP/Ag	17.11	17.80	2022	14
ITO/PTAA/Al_2O_3/PVSK/C_{60}/SnO_2/Ag	12.84	21.07(certified)	2022	15

References

1 Bi, E. *et al.* Efficient Perovskite Solar Cell Modules with High Stability Enabled by Iodide Diffusion Barriers. *Joule* **3**, 2748-2760 (2019).

2 Chen, S. *et al.* Stabilizing perovskite-substrate interfaces for high-performance

perovskite modules. *Science* **373**, 902-907 (2021).
3 Chen, S. *et al.* Preventing lead leakage with built-in resin layers for sustainable perovskite solar cells. *Nat. Sustain.* **4**, 636-643 (2021).
4 Chen, S. *et al.* Iodine reduction for reproducible and high-performance perovskite solar cells and modules. *Sci. Adv.* **7** (2021).
5 Chiang, C.-H. *et al.* One-step fabrication of a mixed-halide perovskite film for a high-efficiency inverted solar cell and module. *J. Mater. Chem. A* **4**, 13525-13533 (2016).
6 Chiang, C.-H. *et al.* The synergistic effect of H_2O and DMF towards stable and 20% efficiency inverted perovskite solar cells. *Energy Environ. Sci.* **10**, 808-817 (2017).
7 Deng, Y. *et al.* Tailoring solvent coordination for high-speed, room-temperature blading of perovskite photovoltaic films. *Sci. Adv.* **5**, eaax7537 (2019).
8 Heo, J. H. *et al.* Hysteresis-less inverted $CH_3NH_3PbI_3$ planar perovskite hybrid solar cells with 18.1% power conversion efficiency. *Energy Environ. Sci.* **8**, 1602-1608 (2015).
9 Hu, J. *et al.* Spontaneously Self-Assembly of a 2D/3D Heterostructure Enhances the Efficiency and Stability in Printed Perovskite Solar Cells. *Adv. Energy Mat.* **10**, 2000173 (2020).
10 Li, J. *et al.* A Regularity-Based Fullerene Interfacial Layer for Efficient and Stable Perovskite Solar Cells via Blade-Coating. *Adv. Funct. Mater.* **32**, 2105917 (2021).
11 Meng, X. *et al.* Bio-inspired vertebral design for scalable and flexible perovskite solar cells. *Nat. Commun.* **11**, 3016 (2020).
12 Seo, J. *et al.* Benefits of very thin PCBM and LiF layers for solution-processed p–i–n perovskite solar cells. *Energy Environ. Sci.* **7**, 2642-2646 (2014).
13 Xue, T. *et al.* Mechanically Robust and Flexible Perovskite Solar Cells via a Printable and Gelatinous Interface. *ACS Appl. Mater. Interfaces* **13**, 19959-19969 (2021).
14 Zeng, H. *et al.* Improved Performance and Stability of Perovskite Solar Modules by Regulating Interfacial Ion Diffusion with Nonionic Cross-Linked 1D Lead-Iodide. *Adv. Energy Mat.* **12**, 2102820 (2021).
15 Gao, Y. *et al.* Can Nanosecond Laser Achieve High-Performance Perovskite Solar Modules with Aperture Area Efficiency Over 21%? *Adv. Energy Mater.* 10.1002/aenm.202202287, 2202287 (2022).